

Original Research

Remediation Mechanism and Evaluation for Cd Polluted Vegetable Soil using Palygorskite

Jianrui Li^{1*}, Yingming Xu²¹Taiyuan Institute of Technology, Taiyuan, 030008, China²Agro-Environmental Protection Institute, Ministry of Agriculture and Rural Affairs, Tianjin, 300191, China

Received: 22 April 2024

Accepted: 28 June 2024

Abstract

The field experiments were done to illuminate the remediation mechanisms and effects of palygorskite on Cd (cadmium) polluted vegetable soils. The specific surface area, pore size distribution, X-ray diffraction (XRD) pattern of palygorskite, and X-ray photoelectron spectroscopy (XPS) pattern of Cd adsorption product were characterized to analyze the mechanisms of Cd immobilization by palygorskite. The field trials investigated the influences of palygorskite on pH, CEC (cation exchange capacity), available Cd in soils, concentrations of Cd and sulfur compounds in plants, and enzymatic activity and microbial population in soils. The results showed palygorskite was a hydrated magnesia aluminum silicate clay mineral, with a micropore and mesopore distribution and a specific surface area of 135.7 m²/g. The available Cd in soils was reduced by 11.8%-49.0% after 0.5%-3.0% palygorskite application, accompanied by 9.3%-55.8% reduction of Cd in the shoot of the plant ($p < 0.05$). The rise in pH of 0.06-0.90 units and maximum increase of 19.5% for CEC in treated soils were conducive to a decline in Cd availability in soils ($p < 0.05$). The 21.8%–50.6% increase for GSH (glutathione) and 22.7%–44.6% for PCs (plant chelating peptides) in shoots were observed in treated soils to upgrade the ability of plants to resist Cd-induced oxidative stress. The changes in enzymatic activity and microbial number demonstrated the recovery of microbial functions that occurred in amended soils. The palygorskite application in a Cd polluted vegetable field was practicable in realizing the safety regulation of plants and the restoration of soil microbial function.

Keywords: remediation, Cd, vegetable soil, palygorskite

Introduction

16.7% of arable land, approximately 2×10^7 ha, has been contaminated with heavy metals in China. The soil pollution survey by the Ministry of Ecology and Environment revealed that the rate of exceeding

the standard of 0.30 mg/kg (GB15618-2018) in farmland was 19.4%. The vegetable industry has grown from 3.3×10^6 ha in 1978 to 2.2×10^7 ha in 2015 in the process of industrialization and urbanization, accounting for 13% of arable land area. The heavy metals in vegetables mainly originate from soil, irrigation water, agricultural chemicals, and atmospheric deposition [1, 2]. The average content of Cd in vegetable fields was 0.30 mg/kg, exceeding the national background value by 300%. The average concentrations of Pb, Cd,

*e-mail: jianrui-419@163.com

and Hg in vegetables were 0.11, 0.04, and 0.01 mg/kg, respectively. The leafy vegetables were the main source of Cd exposure due to a stronger ability to assimilate Cd compared to varieties of roots and legumes. The safety production of leaf vegetables grown in polluted farmland has become a burning issue of our times [3].

The assimilation and accumulation of heavy metals by leafy vegetables were not only related to their genotype, growth period, and tissue location, but also closely related to soil and environmental factors. Environmental modification has been continuously advancing based on the development strategy of ecological civilization and rural vitalization in China. There have been numerous remediation technologies for heavy metal polluted farmland, including engineering measures, phytoextraction, microbial remediation, and chemical immobilization, in recent years. However, due to issues such as remediation cost and efficiency, there were not many methods that could be widely promoted in practice. The chemical immobilization technology with low cost, fast effectiveness, and easy operation was suitable for the remediation of large areas of medium to light polluted soils and has received widespread attention from environmental researchers [4, 5]. Among amendments of clay minerals, phosphates, and organic matter, clay minerals with high cation exchange capacity and specific adsorption sites have been adopted to remediate heavy metal contaminated farmland due to abundant reserves in nature. The clay minerals such as palygorskite and sepiolite, characterized by negatively charged structure layers, fine grains, and a great specific surface area, could undergo reactions of exchange adsorption, coordination, and co-precipitation with heavy metals, resulting in a reduction of the availability of heavy metals in polluted soils [6, 7].

The scanning electron microscopy (SEM), specific surface area, and pore size distribution of palygorskite were observed to provide information on porous structure, and the mechanisms of Cd immobilization by palygorskite were surveyed by the patterns of X-ray diffraction (XRD) and X-ray photoelectron spectroscopy (XPS) of the Cd adsorbed product in the study. This field experiment investigated the influences of palygorskite application on Cd availability in vegetable soils, Cd accumulation in shoots and roots of plants, sulfur compounds in plants, and plant growth to estimate the ability of plants to resist Cd-induced oxidative stress. The effects of palygorskite addition on factors of Cd availability in soils, including pH and cation exchange capacity (CEC), were studied. The soil fertility index, involving enzymatic activity and microbial population, was evaluated to demonstrate the influences of palygorskite on soil microbial function.

Materials and Methods

Tested Materials

The palygorskite was purchased from Jiangsu Province in China and used as an amendment for the remediation of Cd polluted fields. The palygorskite was a 2:1 hydrated magnesia aluminum silicate clay mineral with a layered chain structure (Fig. 1). The scanning electron microscopy (SEM, ZEISS-Gemini 300) was used to analyze the morphology of the palygorskite samples. The palygorskite showed a great Cd fixation capacity, with pH and CEC of 9.61 and 468.3 mmol/kg, detected using methods provided by Lu [8].

The XRD pattern of palygorskite and XPS pattern of Cd adsorption product were made pertinent characterization in order to investigate the chemical pathways of cadmium immobilization by palygorskite. The 1.00 g palygorskite sample passing through a 0.075 mm sieve was mixed with 200 ml of CdCl₂ solution with a Cd concentration of 50 mg/l at 25°C and then stirred at a speed of 160 rpm for 24 h to finish the Cd adsorption experiment.

The XRD patterns were recorded on a Bruker/D8 Advance X-ray diffractometer operated at 60 kV and 80 mA using Cu-K α radiation at a scanning speed of 2.0°/min over 2 θ from 5° to 40°. The XPS spectra were recorded using an ESCALAB 250xi spectrometer employing a monochromatic Al-K α X-ray source (h ν = 1486.6 eV). The X-ray gun operated at a power of 15 kV \times 10 mA with a background vacuum of 1 \times 10⁻⁸ Pa in the analysis room. The nonlinear multi peak fitting by Gaussian curve was made for a fine spectrum of cadmium and carbon elements. The XPS survey spectra were recorded with a pass energy of 100 eV and high resolution spectra with a pass energy of 50 eV.

The test field was located in a suburb, and soil pollution was primarily caused by the introduction of municipal domestic sewage and industrial effluent. The total content of Cd in the vegetable field was 1.53 mg/kg, higher than the Chinese standard GB 15618-2018 of 0.30 mg/kg. The pH and CEC of the soil sample were 6.03 and 113.7 mmol/kg, respectively. The average bulk density in the 0-20 cm soil layer was about 1.0 g/cm³. The tested leaf vegetable of cabbage (Jinqing No.2) was a common cultivated variety in the local area, and the average growth period of the plant was 70 d.

Experimental Design

The palygorskite was evenly applied to topsoil of 0-20 cm at dosages of 0, 1.0 (0.5%), 2.0 (1.0%), 3.0 (1.5%), 4.0 (2.0%), 5.0 (2.5%), and 6.0 kg/m² (3.0%) in the test plot in April 2023. The seeds of the plant were sterilized in 2% (v/v) H₂O₂ for 20 min and soaked in water for 24 h. The soaked seeds were then sown in unpolluted soils, and seedlings of the plant after 20 d

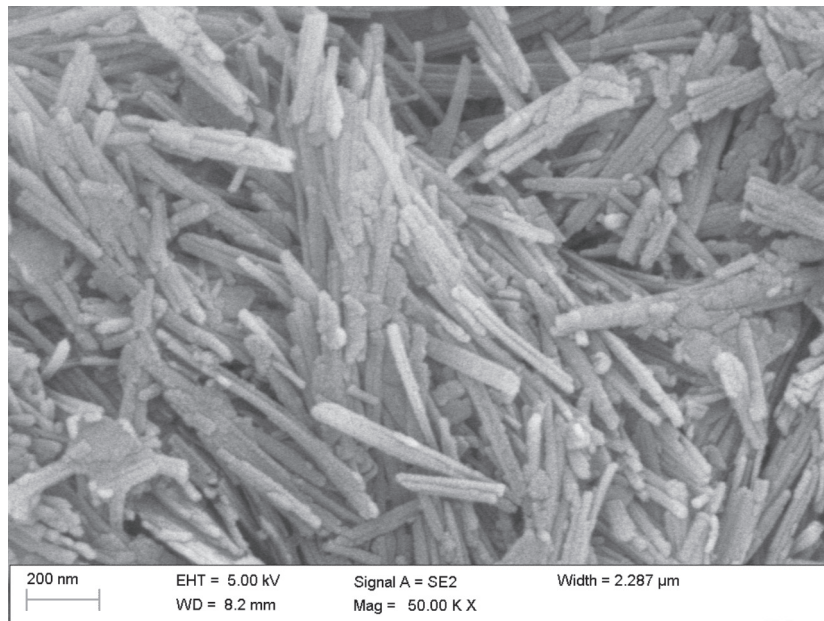


Fig. 1. The SEM (scanning electron microscopy) pattern of palygorskite.

of growth were transplanted in each plot of 5 m × 6 m with a planting density of 4 strains/m² in May 2023. The plots were arranged in a randomized block, and the protection rows were set up in a field test. The plots were surrounded by ridges covered with plastic film to prevent cluster irrigation between plots. The vegetable was harvested in July 2023. The plum blossom type of sampling was adopted to collect plant samples. The rhizosphere soil was separated from the root by shaking off soil attached to the root. The tissues of the shoot and root were air-dried and dried to a constant weight at 70°C. The plant sample was ground with a stainless mill and passed through a 0.25 mm sieve before a chemical test. The soil sample passing through a 2.0 mm sieve was used to do the analysis of pH and available Cd.

Analytical Methods

The characterizations of BET surface area and pore size distribution of palygorskite based on N₂ adsorption and desorption isotherms were implemented using a DFT calculation model of N₂ at 77 K on carbon (slit pore, NLDFT equilibrium model). The parameters, including an N₂ adsorption temperature of 77.350k, an outgas temperature of 100°C, an adsorption time of 1045.1 min, and outgas time of 60.0 min, palygorskite weight of 0.3964g in the sample tube, liquid nitrogen density of 0.808 g/cm³ and molecule weight of 28.013, and cross section of 16.200Å², were adopted in isothermal adsorption and desorption tests by an adsorption instrument (Quantachrome, Autosorb-iQ).

The pH of the soil sample and palygorskite was determined using a pH meter (PHS-3C, Lei-ci) at a ratio of water to soil of 2.5. The CEC was tested using the sodium acetate (NaOAc) exchange method [8].

The content of available Cd in soils was evaluated using 0.10 mol/l HCl extraction solution. The 5.0 g soil sample was dispersed into a 25 ml HCl solution and then shaken at 110 rph for 60 min, and the concentrations of Cd in the supernatant after filtration were tested by an atomic absorption spectrometer (AA-6880, Shimadzu).

The samples of plant and soil were digested with a solution of HNO₃ and HNO₃-HF, respectively. The certified reference materials of polluted soil (GBW08303) and bush leaf (GBW08612) were used for quality control during the process of digestion.

The 0.10 g harvested plant sample was immediately stored in liquid nitrogen and crushed into a smooth powder. The uniformly mixed sample solution included a plant sample, 1.0 ml of 0.1% TFA (trifluoroacetic acid), and 1.0 ml of 6.3 mmol/l DTPA (diethylenetriamine pentaacetic acid). The above-mentioned sample solution was centrifuged at 12000 rpm and 4.0°C for 10 min, and then the supernatant was utilized to make a test of the contents of glutathione (GSH) and plant chelating peptides (PCs) in the plant sample using the Test Kit (Fantai, Shanghai).

The activity of phosphatase in soils was tested with sodium bis (p-nitrophenyl) phosphate as substrate, incubating at pH 14.0 and 30°C for 10 min, and the residual substrate was detected by the colorimetric method [9]. The activity of invertase in soils was determined using sucrose solution as substrate, incubating at pH 5.5 and 37°C for 24 h, and the produced glucose was detected by the colorimetric method [10]. The dilution plate technology was adopted for microbial population evaluation [11]. The bacterium-mixing plate was utilized, and 10⁻⁵-10⁻⁷ dilutions of soil samples were used as inoculums, and the colonies were counted after culture at 30°C for 3 days. The medium formulation for bacteria of beef extract 5.0 g, peptone 10.0 g, NaCl 5.0 g,

pure water 1.0 l, agar 17.0 g, and pH 7.2-7.4 was set in the test. The fungi-mixing plate was used and 10^{-1} - 10^{-3} dilutions of samples were used as inoculums, and the colonies were determined after culture at 30°C for 3 days. The medium formulation for fungi of glucose 10.0 g, K_2HPO_4 1.0 g, $MgSO_4 \cdot 7H_2O$ 0.5 g, pure water 1.0 l, agar 17.0 g, and pH 4.0-5.0 was designed in the experiment.

Data Analysis

All treatments in the experiments were replicated three times. The means, standard deviations, and analysis of variance were calculated by Microsoft Office Excel 2021. The multiple comparisons were made using the least significant difference (LSD) test when significant differences were observed among different treatments ($p < 0.05$). The data analysis of XRD was used in Jade 6.5 and XPS data processing for Avantage 5.5. The multiple linear regression analysis was made using Origin 2022.

Results

Surface Area and Pore Size Distribution of Palygorskite

The specific surface area and pore nature of palygorskite were determined using BET measurement. As reported in Fig. 2, the N_2 adsorption and desorption isotherm showed a type IV mode. The adsorption hysteresis characterized by higher adsorption quantity in the desorption branch than in the adsorption branch was observed in the isotherm at a relative pressure of 0.7-1.0. The capillary condensation phenomenon provided the explanation of adsorption hysteresis. The adsorption saturation was not found in high relative pressure, revealing multi-layer adsorption.

As reflected in Fig. 3, the pore size of palygorskite took on a distribution of micropores and mesopores. The specific surface area of palygorskite was $135.7 \text{ m}^2/\text{g}$. The cumulative surface area of micropores accounted for 70.4% of the total surface area, and the surface area of mesopores contributed 29.6% of the sum. Obviously, there was a negative correlation between pore size and specific surface area. As shown in Fig. 4, the total pore volume of palygorskite was $0.2275 \text{ cm}^3/\text{g}$. The cumulative volume of micropores was $0.0409 \text{ cm}^3/\text{g}$, 18.0% of the total pore volume. The 82.0% of pore volume was mainly occupied by mesopores, indicating a leading role of mesopores in pore size distribution.

Cd Immobilization by Palygorskite

The XRD pattern of palygorskite was reported in Fig. 5. The characteristic diffraction peak of the crystal plane $(Mg_5(Si,Al)_8O_{20}(OH)_2 \cdot 8H_2O)$, JCPDS No.31-0783

was detected at $2\theta=8.42^\circ$ (110 reflections), and other characteristic diffraction peaks were found at $2\theta=26.69^\circ$ and $2\theta=31.01^\circ$, reflecting the presence of quartz (SiO_2) and dolomite ($CaMg(CO_3)_2$) in palygorskite. Comparable conclusions were drawn in related research on crystal

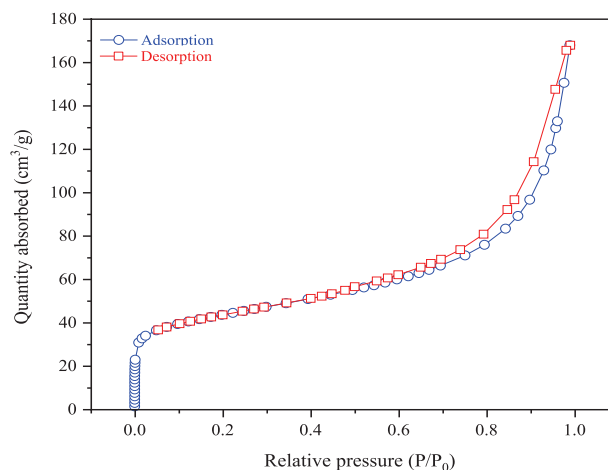


Fig. 2. The isotherm for N_2 adsorption and desorption on palygorskite.

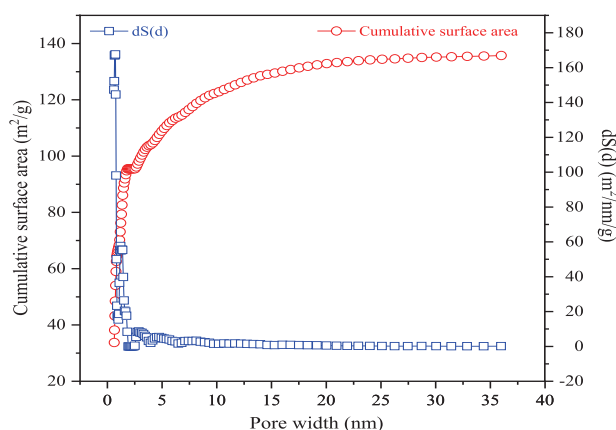


Fig. 3. The analysis of specific surface area of palygorskite.

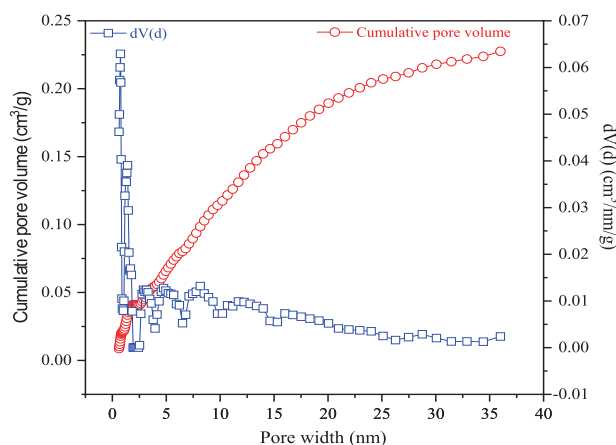


Fig. 4. The pore size distribution of palygorskite.

structure and adsorption experiments of palygorskite [12, 13].

The Cd3d spectra of Cd adsorbed palygorskite were revealed in Fig. 6. The peaks at 406.4 eV and 406.1 eV for Cd3d_{5/2} spectra were detected, revealing the new phase formation of Cd(OH)₂ by complexation between Cd(II) and silanol groups (Si-OH) on the surface of palygorskite. Similar results were obtained in studies of Cd adsorption onto montmorillonite and Cd fixation by palygorskite [12, 14]. The Mg(II) in the pore solution substituted the Al(III) in the octahedral of montmorillonite, gradually transforming from layered montmorillonite to chain layered palygorskite. The presence of hydroxyl and deprotonated hydroxyl groups on the surface of palygorskite was

conducive to the formation of inner-sphere and outer-sphere complexes with Cd(II) [15]. In addition, the peak at 405.7 eV was ascribed to CdCl₂ as the background composition in the initial adsorption solution [7].

The Cl1s spectra of the Cd adsorbed product are shown in Fig. 7, and three characteristic peaks were separated. The peaks at 284.5 eV and 286.4 eV were respectively attributed to the elemental carbon and organic carbon [16, 17]. The peak at 289.6 eV corresponding to CdCO₃ was detected [18], which was due to a chemical reaction between Cd(II) and carbonate (CO₃²⁻) from the dolomite present in palygorskite, as reflected in Fig. 5. The dolomite belonged to the carbonate mineral of the trigonal system.

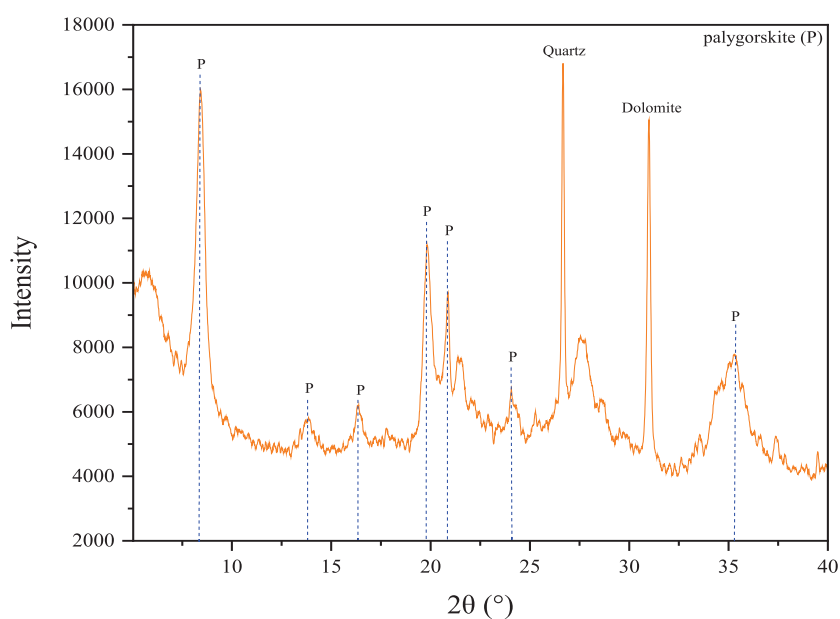


Fig. 5. The XRD (X-ray diffraction) pattern of palygorskite.

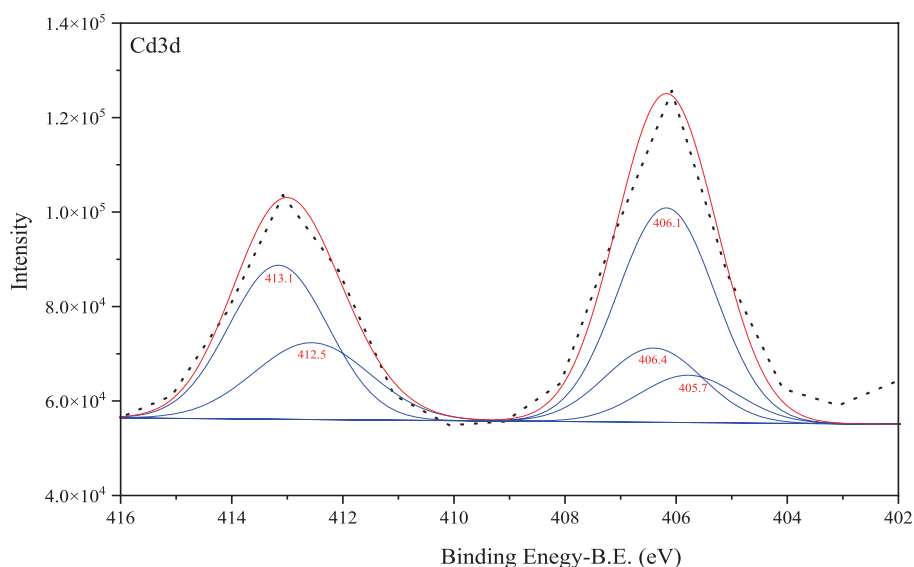


Fig. 6. The Cd3d spectra of Cd adsorbed palygorskite.

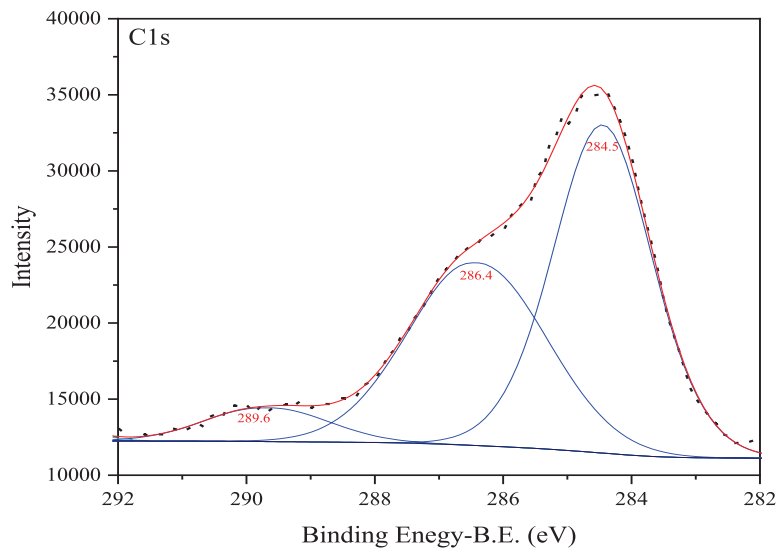


Fig. 7. The C1s spectra of Cd adsorbed palygorskite.

pH, CEC, and Available Cd in Soils

The pH controlled the equilibrium of reactions of oxidation and reduction, precipitation and dissolution, and adsorption and desorption for trace elements in soils and posed a critical influence on heavy metal availability [19, 20]. The effects of palygorskite on pH are shown in Fig. 8. The pH increased by 0.06-0.90 units after 0.5%-3.0% application. The pH rise was mainly caused by the alkaline characteristics of palygorskite.

The CEC was generally affected by the contents of oxide colloids, clay colloids, and organic colloids present in soils, reflecting the capacity of exchange on metal cations. The CEC variation controls the Cd adsorption on colloid and Cd availability. As reported in Fig. 8, the

CEC rose gradually with the different treatments, with a 19.5% increase compared to untreated soil ($p < 0.05$). The palygorskite addition increased the content of clay colloids, resulting in higher CEC.

The mobility and availability of heavy metals in soils were strongly dependent on pH, and the metal availability declined gradually as the pH increased. The increases in pH and Cd absorption on colloids caused the reduction of Cd availability in treated soils. In soils untreated with palygorskite, as shown in Table 1, the available Cd accounted for 33.3% of total Cd in soils. The percentage of available Cd was inhibited in treated soils, and the available Cd was reduced by 11.8%-49.0% at an applied dose of 0.5%-3.0% ($p < 0.05$).

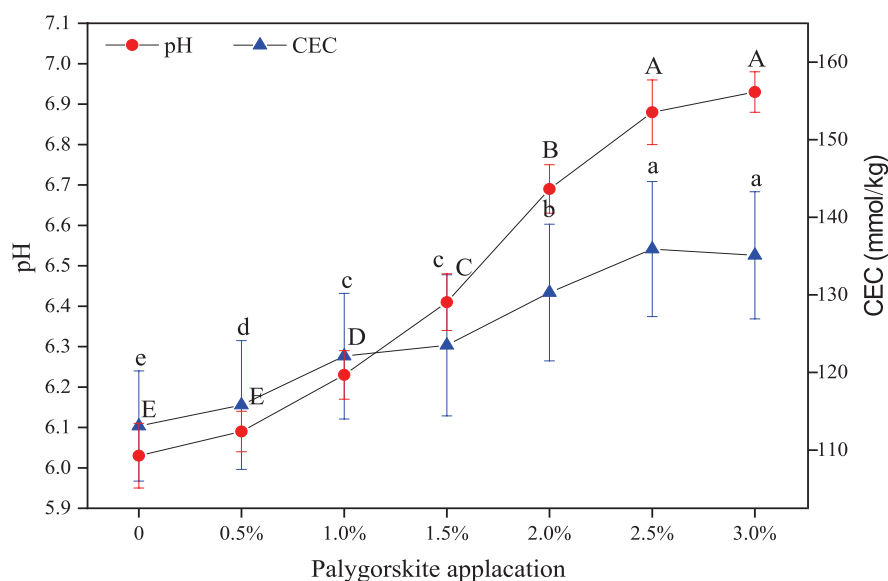


Fig. 8. The pH and CEC (cation exchange capacity) in soils. The means with different letters were significantly different from each other at different palygorskite addition ($n = 3$, $p < 0.05$).

Table 1. The available Cd, activities of enzymes, and microbial population in soils.

Palygorskite application	Available Cd (mg/kg)	Enzymatic activities		Microbial population	
		Invertase (mg/g/h)	Phosphatase (mg/g/h)	Bacteria (10^7 CFU/g)	Fungi (10^5 CFU/g)
0	0.51±0.05a	3.1±0.16a	4.2±0.26d	1.13±0.08f	1.81±0.21a
0.5%	0.45±0.04b	3.2±0.21a	4.3±0.31d	1.26±0.07e	1.75±0.23ab
1.0%	0.41±0.05bc	3.2±0.23a	4.6±0.25c	1.41±0.13d	1.69±0.19b
1.5%	0.36±0.04c	3.0±0.18a	5.2±0.28b	1.55±0.09c	1.70±0.18b
2.0%	0.35±0.06c	3.3±0.16a	5.1±0.25b	1.73±0.15b	1.56±0.25c
2.5%	0.30±0.03d	3.0±0.15a	5.8±0.33a	1.66±0.11b	1.47±0.22d
3.0%	0.26±0.03e	3.1±0.15a	5.7±0.32a	1.82±0.12a	1.36±0.16e

Note: Different letters in the column were significantly different ($p < 0.05$; LSD test).

Biomass and Concentration of Cd of Plant

Excessive Cd can interfere with the absorption and distribution of mineral nutrients, and the structure and development of plant cells are damaged, causing plant growth disorders. The variation of biomass could serve as an index for the toxicity of Cd to plants. The palygorskite application improved the plant growth, as reported in Fig. 9. Although 2.5%-3.0% palygorskite treatment decreased the shoot biomass, the biomass under 0.5%-2.0% addition was enhanced by 13.7%-35.3% ($p < 0.05$). The reductions of shoot biomass at 2.5-3.0%, as the pH increased, were possibly caused by the declines in available concentrations of macroelements (potassium) and microelements (copper, zinc, etc.) in treated soils. The macroelement and microelement were components of metabolic enzymes in plants, which were necessary for redox reactions, protein

synthesis, photosynthesis, carbohydrate formation and migration, and reproductive organ development. Obviously, a moderate dose should be recommended to promote plant growth. The root biomass in treated soils showed increases of 7.0%-70.8% ($p < 0.05$). The increasing biomass of plants could predict a reduction of Cd phytotoxicity.

The concentrations of Cd in the shoot and the root of the plant were lined in Fig. 10. Generally, the concentration of Cd in the root was much higher than that in the shoot. In untreated soils, the content of Cd in shoots was far beyond the guideline of 0.20 mg/kg (GB2762-2012). The Cd in shoots in amended soils reduced by 9.3%-55.8% ($p < 0.05$). The Cd in shoots was lower than 0.20 mg/kg when the applied dose exceeded 3.0%, achieving the safe production of the plant. The palygorskite addition remarkably decreased the Cd in the root, leading to 9.9%-58.0% ($p < 0.05$).

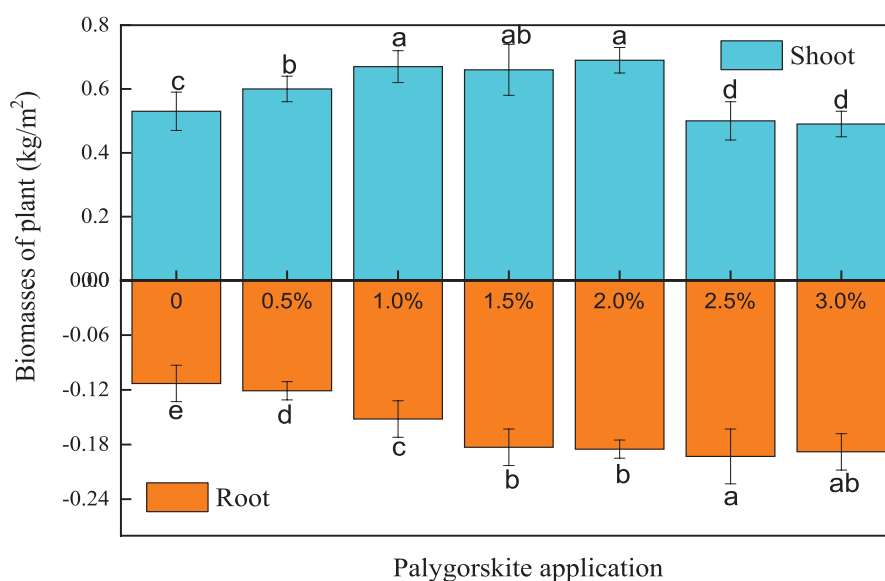


Fig. 9. The biomasses of different parts of plant. The same letters above bars were not significantly different at different palygorskite addition ($n = 3$, $p < 0.05$).

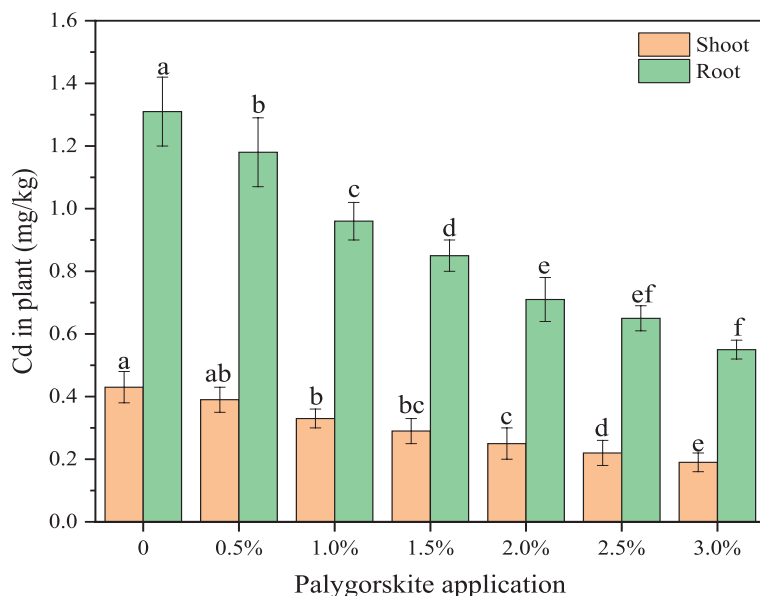


Fig. 10. The concentrations of Cd in different parts of plant. The same letters above bars were not significantly different at different palygorskite addition ($n = 3, p < 0.05$).

Contents of Sulfur Compounds in Root and Shoot

The Cd toxicity caused the accumulation of reactive oxygen species and oxidative stress in plant cells, which could attack lipids, proteins, pigments, and riboacids, leading to lipid peroxidation, enzyme activity inhibition, cell fluidity disorder, and damage to cell membranes and organelles. The Cd oxidative stress activated the detoxification pathways in plant cells, and the increased synthesis of sulfur compounds, glutathione (GSH), and plant chelating peptides (PCs), was an important mechanism for tolerance and detoxification. The GSH and plant PCs were ideal ligands for Cd^{2+} , enhancing the

ability of plant cells to resist oxidative stress. Notably, plant chelating peptide cadmium complexes can enter vacuoles through ATP transporters on the vacuole membrane, reducing intracellular Cd toxicity [21].

The contents of GSH and PCs in shoots and roots in different treatments were reported in Fig. 11. In general, higher GSH and PC contents in shoots than in roots were observed. The palygorskite application increased the contents of GSH and PCs in roots by 7.7%-34.1% and 4.5%-33.3% in contrast to treatments with no clay. As for shoots, palygorskite additions led to an increase in GSH of 21.8%-50.6% and a raise of 22.7%-44.6% for PCs, respectively.

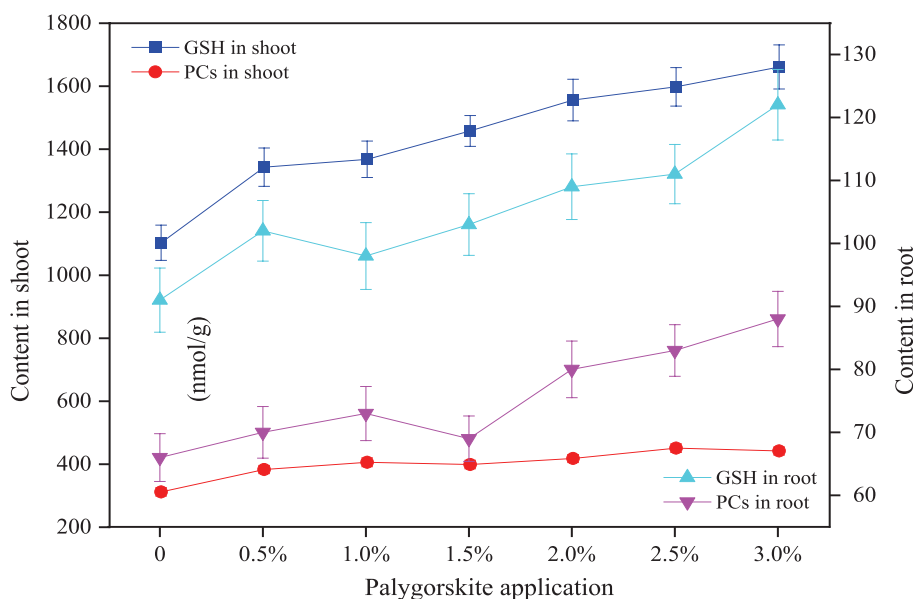


Fig. 11. The contents of GSH and PCs in shoot and root of plant. The GSH and PCs mean glutathione and plant chelating peptides.

Enzymatic Activity and Microbial Population in Soils

The enzymatic activity can act as an indices of fertility level, microbial activity, and environmental quality and reflect the degree of heavy pollution in the field. The phosphatase was an enzyme that could catalyze the hydrolysis of phosphate monoester and phosphate diester in soils to form inorganic phosphorus for root uptake. The invertase was an enzyme widely present in soils, which played an important role in increasing soluble nutrients in soils [9, 22]. The enzymatic activity was sensitive to management practice and pollution fluctuation in farmland. As reported in Table 1, the increase in pH and reduction of Cd availability in soils caused the changes in enzymatic activities in different treatments. The activities of phosphatase in palygorskite treated soils were higher than those in treatment without clay, with increases of 2.4%-38.1% in 0.5%-3.0% ($p < 0.05$). However, there were no remarkable differences in invertase activity among different treatments in soils.

The microorganisms were helpful in the formation of soil aggregates and crop growth promoters. The microbial status, as impetuses of organic matter turnover, community stability, and integrity in the soil ecosystem, can be useful in evaluating the remediation efficiency of polluted soils and its influence on the restoration of soil function [23, 24]. As lined in Table 1, palygorskite application promoted the bacteria number, with increases of 11.5%-61.1% ($p < 0.05$). The fungi number after clay mineral addition was inhibited significantly.

Discussion

The acquaintance of soil and plant relationships in a metal polluted vegetable field was a hot issue because of the important role of leaf vegetables in the daily diet. The palygorskite of mesoporous material was an ideal amendment for Cd polluted vegetable soils due to its high specific surface area and CEC (Fig. 3). As shown in Table 1, Fig. 9, and Fig. 10, the 0.5%-2.0% palygorskite application promoted the growth of plants and decreased the available Cd in soils, and the concentration of Cd in the shoots of plants in the 3.0% treatment met the requirement of the national food hygienic standard of 0.20 mg/kg (GB2762-2012).

The fluctuation of Cd availability after palygorskite addition was related to pH and CEC in soils. The available Cd was negatively related to pH ($r = 0.84$) and CEC ($r = 0.57$) in soils.

The available Cd responded more significantly to pH than CEC, and pH rise played a critical role in the reduction of available Cd in treated soils. The pH, CEC, and available Cd in soils were critical impact factors for Cd in shoots of plants, and palygorskite application had an influence on pH, CEC, and available Cd. In order to study the relationship between impact factors of Cd

availability and Cd in the shoot, the multiple linear regression for the effect of pH, CEC, available Cd, and palygorskite application on Cd in the shoot was done. The linear regression equation was $Y = -0.06 X_1 - 0.001 X_2 + 0.92 X_3 + 1.17 X_4 + 0.33$ ($R^2 = 0.98$, $p < 0.05$), X_1 , X_2 , X_3 , and X_4 , and Y represented the pH, CEC, available Cd, palygorskite application, and Cd in the shoot. The ratios of predictive value to the observed value of Cd in a shoot in 0-3.0% treatment were 0.99, 0.96, 1.01, 0.97, 1.04, 0.96, and 0.92. In the future, different types of soil characterized by distinct values of pH, CEC, and available Cd and a rationally applied dose of clay mineral should be recommended to realize the safe production of plants.

The studies have reported additions of palygorskite and sepiolite promoted the Cd form transformation from exchangeable to Fe/Mn oxide bound and residual species, and the contents of CaCl_2 and HCl extractable Cd and DTPA extractable fraction in amended soils declined significantly [7, 25]. The effects of clay application on metal leachability and phytoavailability were assessed by leaching tests and plant experiments in metal polluted mine soils. The leachability of Cd in soils was reduced by 60%-70% after 5% sepiolite addition, and the maximum decrease of trace elements in the shoot of alfalfa was up to 45% [26].

The palygorskite application reduced the oxidative damage of the cell membrane and enhanced the regulatory ability of the antioxidant system to reduce Cd toxicity to plants (Fig. 11). The activities of antioxidant enzymes in leaves of rice plants showed a remarkable rise after applying clay minerals to Cd polluted fields, with 12.7%-47.6% for SOD (superoxide dismutase), 13.2%-57.3% for POD (peroxidase), and 12.3%-42.1% for CAT (catalase) in traditional irrigation, equally reflecting the elevation of plant resistance to Cd oxidative stress [6, 25]. The significant increases in biomass of roots and shoots of the plant, as revealed in Fig. 9, were in part attributed to the rise of GSH and PCs in the plant. The physiological response of plants still requires extensive work for the sustainability of agricultural ecosystems in the future.

The heavy metal can replace metal ions in the active center of the enzyme and inactivate the enzyme. The palygorskite addition decreased the biological toxicity of Cd to enzymes, which was the main reason for the increase in enzymatic activity (Table 1). The pot studies demonstrated that, as the decrease of soil leachable Cd, the activities of catalase in sepiolite combined with bentonite treated soils were stimulated, and the basal soil respiration, dehydrogenase, and alkaline phosphatase activities in soils increased by 25%, 138%, and 42%, which indicated remediation measures improved the soil fertility index and microbial functions [26, 27]. The immobilization remediation of Cd polluted rice fields found that the activities of urease, acid phosphatase, and sucrose in clay treated soils were increased in different degrees, reflecting the metabolic reactions being restored step by step [28].

The enhance values of enzyme activity and microbial population in soils were observed in the field experiment, which demonstrated that the ecological function regained after applying palygorskite to Cd polluted vegetable fields.

Conclusions

The palygorskite was an effective amendment, based on microporous and mesoporous structure and great specific surface area, for immobilization remediation of Cd polluted vegetable fields to reduce the ecological risk of Cd. The Cd immobilization by palygorskite was attributed to the formation of Cd(OH)₂ between Cd(II) and hydroxyl groups (Si-OH) on the surface of palygorskite, as well as CdCO₃ generation between Cd(II) and carbonate present in palygorskite. The amendment addition decreased the available Cd in vegetable soils and the concentration of Cd in plants. The contents of sulfur compounds of GSH (glutathione) and PCs (plant chelating peptides) in plants in treated soils rose significantly to improve the ability of plants to resist Cd-induced oxidative stress. The reduction of available Cd in amended soils was due to increases in pH and cation exchange capacity (CEC). The values of enzymatic activity and microbial population in vegetable soils were enhanced after palygorskite addition, reflecting the increase in soil fertility and microbial function.

Acknowledgments

This work was supported by Fundamental Research Program of Shanxi Province (No. 202203021221232). We thank for the financial backing.

Conflict of Interest

The authors declare no conflict of interest.

References

- HUANG Y., CHEN Q.Q., DENG M.H., JAPENGA J., LI T.Q., YANG X.E., HE Z.L. Heavy metal pollution and health risk assessment of agricultural soils in a typical peri-urban area in southeast China. *Journal of Environmental Management*, **207**, 159, **2018**.
- WANG Y.R., WANG R.M., FAN L.Y., CHEN T.T., BAI Y.H., YU Q.R., LIU Y. Assessment of multiple exposure to chemical elements and health risks among residents near Huodehong lead-zinc mining area in Yunnan, Southwest China. *Chemosphere*, **174**, 613, **2017**.
- HU N.W., YU H.W., DENG B.L., HU B., ZHU G.P., YANG X.T., WANG T.Y., ZENG Y., WANG Q.Y. Levels of heavy metal in soil and vegetable and associated health risk in peri-urban areas across China. *Ecotoxicology and Environmental Safety*, **259**, 115037, **2023**.
- YAO A.J., WANG Y.N., LING X.D., CHEN Z., TANG Y.T., QIU H., YING R.R., QIU R.L. Effects of an iron-silicon material, a synthetic zeolite and an alkaline clay on vegetable uptake of As and Cd from a polluted agricultural soil and proposed remediation mechanisms. *Environmental Geochemistry and Health*, **39** (2), 353, **2017**.
- WANG Y.L., XU Y.M., LIANG X.F., WANG L., SUN Y.B., HUANG Q.Q., QIN X., ZHAO L.J. Soil application of manganese sulfate could reduce wheat Cd accumulation in Cd contaminated soil by the modulation of the key tissues and ionic of wheat. *Science of The Total Environment*, **770**, 145328, **2021**.
- LI J.R., XU Y.M. Influence of clay application and water management on ability of rice to resist cadmium stress. *Environmental Engineering Science*, **38** (7), 695, **2021**.
- LIANG X.F., HAN J., XU Y.M., SUN Y.B., WANG L., TAN X. In situ field-scale remediation of Cd polluted paddy soil using sepiolite and palygorskite. *Geoderma*, **235–236**, 9, **2014**.
- LU R.K. *Analysis Methods of Soil Agricultural Chemistry*, 2nd ed.; Chinese Agricultural Science Technology Press: Beijing, China, pp. 152-177, **2000** [In Chinese].
- WANG Q.Y., SUN J.Y., HU N.W., WANG T.Y., YUE J., HU B., YU H.W. Effects of soil aging conditions on distributions of cadmium distribution and phosphatase activity in different soil aggregates. *Science of The Total Environment*, **834**, 155440, **2022**.
- YU Z.J., LIU X.D., ZENG X.B., YIN H.Q., YU R.L., ZENG W.M. Effect of arsenic pollution extent on microbial community in shimen long-term arsenic-contaminated soil. *Water, Air, & soil pollution*, **231** (7), 340, **2020**.
- GUO L., WANG C., FENG T.Y., SHEN R.F. Short-term application of organic fertilization impacts phosphatase activity and phosphorus-mineralizing bacterial communities of bulk and rhizosphere soils of maize in acidic soil. *Plant and Soil*, **484** (1-2), 95, **2023**.
- CHEN Z.X., CHEN C.S., CHEN W.P., JIAO W.T. Effect and mechanism of attapulgite and its modified materials on bioavailability of cadmium in soil. *Environmental Science*, **39** (10), 4744, **2018** [In Chinese].
- LIU H.B., CHEN T.H., CHANG D.Y., CHEN D., QING C.S., XIE J.J., FROST R.L. The difference of thermal stability between Fe-substituted palygorskite and Al-rich palygorskite. *Journal of Thermal Analysis and Calorimetry*, **111** (1), 409, **2013**.
- KIM S.H., HEO N.H., KIM G.H., HONG S.B., SEFF K. Preparation, crystal structure, and thermal stability of the cadmium sulfide nanoclusters Cd₆S₄⁴⁺ and Cd₂Na₂S₄⁺ in the sodalite cavities of zeolite A (LTA). *Journal of Physical Chemistry B*, **110** (51), 25964, **2006**.
- NEAMAN A., SINGER A. The effects of palygorskite on chemical and physico-chemical properties of soils: a review. *Geoderma*, **123** (3-4), 297, **2004**.
- KLOPROGGE J.T., WOOD B.J. Baseline studies of the clay minerals society source clays by X-ray photoelectron spectroscopy. *Clay Science*, **22** (4), 85, **2018**.
- POWELL C.J. Recommended Auger parameters for 42 elemental solids. *Journal of Electron Spectroscopy and Related Phenomena*, **185** (1-2), 1, **2012**.
- HAMMOND J.S., GAARENSTROOM S.W., WINOGRAD N. X-ray photoelectron spectroscopic studies of cadmium–oxygen and silver–oxygen surfaces. *Analytical Chemistry*, **47** (13), 2193, **1975**.
- FENG X.Y., WANG Q.L., SUN Y.H., ZHANG S.W., WANG F.Y. Microplastics change soil properties, heavy metal availability and bacterial community in a Pb-Zn-

- contaminated soil. *Journal of Hazardous Materials*, **424**, 127364, **2022**.
20. AKOTO R., ANNING A.K. Heavy metal enrichment and potential ecological risks from different solid mine wastes at a mine site in Ghana. *Environmental Advances*, **3**, 100028, **2021**.
21. ZHANG S.N., HUANG Y.Z., LI Y., BAO Q.L., HUANG Y.C. Effects of different exogenous plant hormones on the antioxidant system and Cd absorption and accumulation of rice seedlings under Cd stress. *Environmental Science*, **42** (4), 2040, **2021** [In Chinese].
22. BARBOSA J.Z., POGGERE G., CORRÊA R.S., HUNGRIA M., MENDES I.D.C. Soil enzymatic activity in Brazilian biomes under native vegetation and contrasting cropping and management. *Applied Soil Ecology*, **190**, 105014, **2023**.
23. ZHU Q.R., YANG Z.Y., ZHANG Y.P., WANG Y.Z., FEI J.C., RONG X.M., PENG J.W., WEI X.M., LUO G.W. Intercropping regulates plant- and microbe-derived carbon accumulation by influencing soil physicochemical and microbial physiological properties. *Agriculture, Ecosystems & Environment*, **364**, 108880, **2024**.
24. LU J.H., LIU Y.X., ZOU X.X., ZHANG X.J., YU X.N., WANG Y.F., SI T. Rotational strip peanut/cotton intercropping improves agricultural production through modulating plant growth, root exudates, and soil microbial communities. *Agriculture, Ecosystems & Environment*, **359**, 108767, **2024**.
25. YIN X.L., XU Y.M., HUANG R., HUANG Q.Q., XIE Z.L., CAI Y.M., LIANG X.F. Remediation mechanisms for Cd-contaminated soil using natural sepiolite at the field scale. *Environmental Science - Processes & Impacts*, **19** (12), 1563, **2017**.
26. VALLE P.A., AYUSO E.Á., MURCIEGO A., PELLITERO E. Assessment of the use of sepiolite amendment to restore heavy metal polluted mine soil. *Geoderma*, **280**, 57, **2016**.
27. SUN Y.B., SUN G.H., XU Y.M., LIU W.T., LIANG X.F., WANG L. Evaluation of the effectiveness of sepiolite, bentonite, and phosphate amendments on the stabilization remediation of cadmium-contaminated soils. *Journal of Environmental Management*, **166**, 204, **2016**.
28. LI J.R., XU Y.M. Effects of clay combined with moisture management on Cd immobilization and fertility index of polluted rice field. *Ecotoxicology and Environmental Safety*, **158**, 182, **2018**.